

# Roles of Surface and Bulk Lattice Oxygen in Forming CO<sub>2</sub> and CO During Methane Reaction over Gadolinia-Doped Ceria

Ta-Jen Huang · Chun-Hsiu Wang

Received: 15 May 2007 / Accepted: 3 June 2007 / Published online: 22 June 2007  
© Springer Science+Business Media, LLC 2007

**Abstract** Temperature-programmed reaction of methane and temperature-programmed reduction were performed over gadolinia-doped ceria (GDC). It was found that CO<sub>2</sub> formation can occur at very much lower temperature than CO formation. The surface lattice oxygen acts as the active site for CH<sub>4</sub> adsorption. This active site has a dynamic characteristic due to the mobility of the lattice oxygen. The rates of CO and CO<sub>2</sub> formations can be controlled by the supply rate of the lattice oxygen from the GDC bulk; this supply rate depends on the mobility and the concentration of the bulk lattice oxygen. CO<sub>2</sub> formation is associated with the existing surface lattice oxygen while CO formation depends on the oxygen species coming from the bulk lattice during methane reaction.

**Keywords** Methane reaction · Carbon dioxide · Carbon monoxide · Gadolinia-doped ceria · Lattice oxygen

## 1 Introduction

Gadolinia-doped ceria (GDC) has been frequently used as the ceramic component in the anode cermet materials for solid oxide fuel cells (SOFCs) operating on methane [1–5]. For methane reactions over high temperature SOFC anodes, especially in the direct-methane SOFCs, carbon deposition (coking) is usually a problem and can cause cell failure [6]; however, the coking problem can be avoided if GDC is used as the anode materials without metal [7, 8]. In

these methane reactions, the lattice oxygen of GDC has exhibited important roles [5, 9]. A new phenomenon of electrochemical promotion of lattice oxygen extraction from GDC bulk has been observed in the direct-methane SOFCs for the cogeneration of synthesis gas [10].

For methane reactions in the direct-methane SOFCs [11, 12], the formation of only CO but not CO<sub>2</sub> should lead to a large difference in the fuel efficiency for power generation. This is due to that the electrochemical formation of CO<sub>2</sub> involves four electrons while that of CO involves only two electrons, with each oxygen ion carrying two electrons; thus, the current density with CO<sub>2</sub> formation is two times that with CO formation in terms of the utilization of carbon in methane. On the other hand, when the direct-methane SOFCs are employed to carry out the cogeneration of synthesis gas, i.e., CO plus hydrogen, the formation of only CO but not CO<sub>2</sub> is preferred. Therefore, it has some importance to study the role of the lattice oxygen, either at the surface or in the bulk, in forming CO<sub>2</sub> and CO during methane reactions over GDC, a mixed ionic-electronic conductor (MIEC) [13].

One characteristic of the MIEC materials is the oxygen-ion conductivity, i.e., the mobility of the lattice oxygen; this is also the characteristic of the oxygen-ion conducting materials. Marchetti and Forni [14] reported that the lattice oxygen species of perovskites, the MIEC materials, become available at high temperature and boost the catalytic activity of methane combustion. For the direct-methane SOFCs, the electrochemical methane reaction over the anode uses the lattice oxygen transported from the cathode three-phase boundary through the electrolyte bulk to the anode surface. Thus, the role of the bulk lattice oxygen on the formation of CO or CO<sub>2</sub> during methane reaction should be interesting to be investigated. However, the role of the lattice oxygen, either at the surface or in the bulk of

T.-J. Huang (✉) · C.-H. Wang  
Department of Chemical Engineering,  
National Tsing Hua University, Hsinchu 300, Taiwan, ROC  
e-mail: tjhuang@che.nthu.edu.tw

the MIEC or oxygen-ion conducting materials, in forming  $\text{CO}_2$  and  $\text{CO}$  has not yet been clarified.

The main purposes of this work is the clarification of the roles of the surface and bulk lattice oxygen in forming  $\text{CO}_2$  and  $\text{CO}$  during methane reactions over GDC in the absence of gas-phase oxygen, i.e., a situation related to the direct-methane SOFCs. Notably, GDC is a member of the doped-ceria family and of the MIEC materials, which have gained increasing importance as the materials of electrolyte and electrodes in SOFCs.

## 2 Experimental

### 2.1 Preparation of Gadolinia-doped Ceria

Gadolinia-doped ceria (GDC) was prepared by a co-precipitation method. The details of the method have been reported elsewhere [15]. The prepared GDC was  $(\text{GdO}_{1.5})_{0.1}(\text{CeO}_2)_{0.9}$ . The calcinations of the GDC powders were carried out by heating in air at a rate of  $10^\circ\text{C}/\text{min}$  to  $300^\circ\text{C}$  and held for 2 h, and then to  $700^\circ\text{C}$  and held for 4 h, and then slowly cooled down to room temperature.

### 2.2 Temperature-programmed Reduction

Temperature-programmed reduction (TPR) was carried out using hydrogen under atmospheric pressure in a continuous flow reactor charged with 100 mg of sample catalyst, which was fixed by quartz wool and quartz sand downstream of the bed. The reactor was made of an 8-mm-ID quartz U-tube imbedded in an insulated electric furnace. A K-type thermocouple was inserted into the catalyst bed to measure and control bed temperature. TPR tests were carried out with 30 mL/min of 10%  $\text{H}_2$  in argon from room temperature to the designated temperature at a rate of  $10^\circ\text{C}/\text{min}$  and then held at the designated temperature, or as described in the text. Some details of the TPR test have been reported elsewhere [16].

### 2.3 Temperature-programmed Reaction of Methane

The temperature-programmed reaction of methane was conducted in the same reactor setup as in the TPR test and also charged with 100 mg of sample catalyst. The gas feed was passed through an oxygen filter to eliminate trace amounts of oxygen.

The test was carried out with or without pre-reduction as stated in the text. The pre-reduction treatment was carried out by 30 mL/min  $\text{H}_2$  at the specified temperature for the designated time. The catalyst was kept in argon flow until the designated test temperature. A mixture of 1%  $\text{CH}_4$  in argon was then fed to the catalyst bed at a flow rate of

20 mL/min, calculated to be a molar rate of methane feed at  $81.3\ \mu\text{mol}/(\text{min g})$  by the ideal gas law, and  $\text{CH}_4\text{-TPR}_x$  started from room temperature to  $880^\circ\text{C}$  at a rate of  $10^\circ\text{C}/\text{min}$  and then held at  $880^\circ\text{C}$  for 1 h before cooled down. The reactor outflow was analyzed on-line by gas chromatograph (China Chromatograph 8900, Taiwan),  $\text{CO-NDIR}$  (Beckman 880), and  $\text{CO}_2\text{-NDIR}$  (Beckman 880).

## 3 Results and Discussion

### 3.1 Temperature-programmed Reaction of Methane

The result of temperature-programmed reaction of methane ( $\text{CH}_4\text{-TPR}_x$ ) over the unreduced GDC is presented in Fig. 1. It is seen that there is a lowest-temperature  $\text{CO}_2$  peak at about  $150^\circ\text{C}$ . This  $\text{CO}_2$  peak almost disappears if GDC has been pre-reduced at  $700^\circ\text{C}$ , shown in Fig. 2. This is due to the disappearance of surface oxygen by the  $700^\circ\text{C}$  pre-reduction as evidenced by the temperature-programmed reduction (TPR) profile shown in Fig. 3. Notably, the lower-temperature TPR peak is considered to be due to the reduction of the surface capping oxygen (the surface oxygen species) [7, 17]. With this lower-temperature TPR peak at about  $480^\circ\text{C}$ , shown in Fig. 3, the  $700^\circ\text{C}$  pre-reduction should have removed almost all existing surface oxygen species, i.e., the oxygen species originally existing at the surface. Notably, also, the surface oxygen species can be replenished from the GDC bulk, as will be discussed in the following. Additionally, Fig. 3 shows that the lower-temperature TPR peak of the second TPR profile almost disappears, indicating again the removal of surface oxygen by the first reduction, similar to the pre-reduction on GDC of Fig. 2. Thus,  $\text{CO}_2$  formation over GDC is associated with surface oxygen. In our case

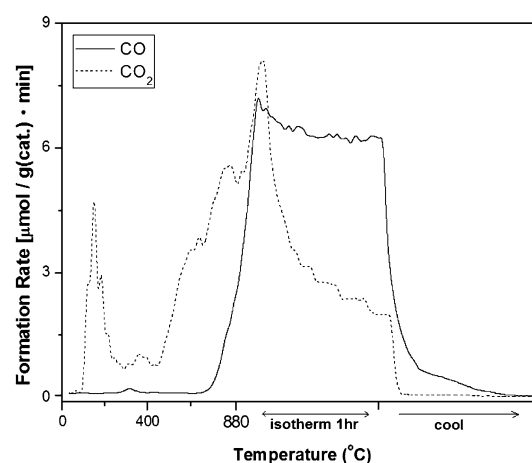


**Fig. 1** Temperature-programmed reaction of methane over unreduced GDC

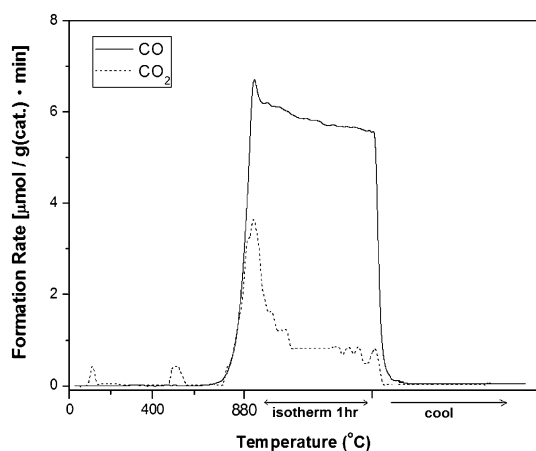


**Fig. 2** Temperature-programmed reaction of methane over GDC pre-reduced at 700 °C for 1 h

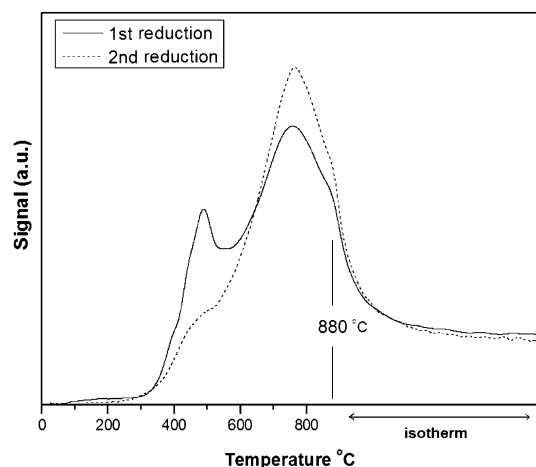


**Fig. 3** Repeated H<sub>2</sub>-temperature-programmed reduction profiles of GDC. The isothermal period during first reduction was 3 h

without gas-phase oxygen, the surface oxygen species is the surface lattice oxygen.

At temperature below about 750 °C, Fig. 1 shows considerable CH<sub>4</sub> oxidation activity, in terms of the rate of carbon oxides formation, but Fig. 2 shows almost no CH<sub>4</sub> activity. As described above, the difference is only the 700 °C pre-reduction, which removed almost all surface lattice oxygen. Thus, it is reasonable to designate the surface lattice oxygen as the active site for CH<sub>4</sub> reaction. CH<sub>4</sub> adsorption may thus be considered as:



where O\* designates the surface lattice oxygen, i.e., the oxygen species in the surface oxygen vacancy. In order to designate O\* as an active site, HO\* instead of OH\* is used for the surface hydroxyl species. Notably, the removal of surface lattice oxygen from ceria may lead to the formation

of surface oxygen vacancies [18]. Notably, also, the surface lattice oxygen may be removed and refilled due to the mobility of the lattice oxygen and thus the active site (O\*) has a dynamic characteristic; that is, if the oxygen species is consumed in the oxidation process but is not replenished, the site of O\* becomes a surface oxygen vacancy and is no longer active for CH<sub>4</sub> adsorption.

Reaction (1) is the oxidative dehydrogenation of methane [19]. The formation of the surface OH species is considered to be via the interaction of the abstracted H species with the surface lattice oxygen [20], or with the oxygen species of the metal oxide as an active site [21]. This is in agreement with the above designation of the surface lattice oxygen as the active site. For CO<sub>2</sub>/CH<sub>4</sub> reforming over high surface area ceria, reaction similar to that of (1) has been proposed; however, the active site has been considered to be either a unique site at CeO<sub>2</sub> surface or a catalytic oxidized site, with the latter formed via oxygen from CO<sub>2</sub> [22]. This could also support the occurrence of reaction (1).

Figure 1 shows also a second CO<sub>2</sub> peak starting at about 400 °C. This is considered to be due to some mobility of bulk lattice oxygen, which enables the bulk lattice oxygen near the surface to be replenished into the surface oxygen vacancy. Consequently, surface lattice oxygen is produced and CO<sub>2</sub> formation can start again. In other words, reaction (1) can occur with the oxygen species coming from the bulk lattice and filling into the surface oxygen vacancies.

Figures 1 and 2 show that, as the temperature increases to about 750 °C, CH<sub>4</sub> reaction over GDC starts to form CO. Since the initial surface lattice oxygen should have been consumed almost completely at 700 °C, the needed surface lattice oxygen for CH<sub>4</sub> adsorption should come from the GDC bulk. Thus, the CO formation rate depends on the supply rate of the oxygen species from the bulk lattice; this supply rate is related to both the mobility and the concentration of the bulk lattice oxygen. During the isothermal period in CH<sub>4</sub>-TPR<sub>x</sub>, with the same reaction temperature and thus the same oxygen mobility, the CO formation rate should be determined by the concentration of bulk lattice oxygen alone. Notably, the mobility of lattice oxygen depends on the temperature. However, Table 1 shows that the total concentration of bulk lattice oxygen of GDC is relatively high and may thus not decrease too much during CO formation. This can explain the behavior of the slowly decreasing CO formation rates during the isothermal period, shown in Figs. 1 and 2.

### 3.2 Temperature-programmed Reduction

The effects of the mobility and the concentration of bulk lattice oxygen on hydrogen consumption during TPR can be revealed by the results of Figs. 3 and 4. It is seen in

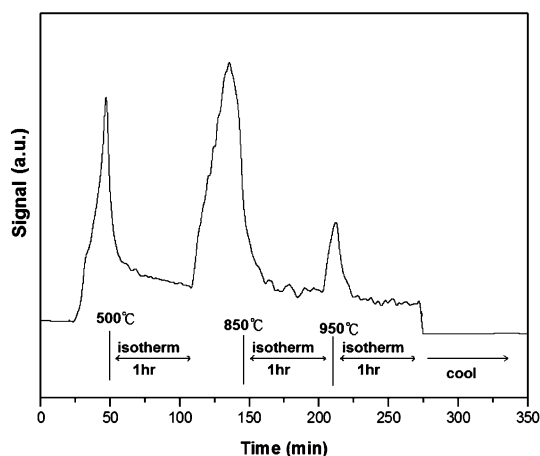
**Table 1** Total amounts of CO<sub>2</sub> and CO formations during temperature-programmed reaction of methane until cooled down

	Total amount in $\mu\text{mol/g GDC}^a$	
	CO <sub>2</sub> Formation	CO Formation
GDC, unreduced	450	408
GDC, 700 °C-reduced 1 h	95	389
GDC, 800 °C-reduced 1 h	176	238
GDC, 900 °C-reduced 1 h	133	73

<sup>a</sup> The total O content in GDC, i.e., (GdO<sub>1.5</sub>)<sub>0.1</sub>(CeO<sub>2</sub>)<sub>0.9</sub>, is 11,270  $\mu\text{mol/g GDC}$

Fig. 3 that the second TPR profile shows a larger higher-temperature peak than that of the first TPR profile. This indicates that, during the first TPR run, only a portion of oxygen species in the bulk lattice was consumed. During the second TPR run, the higher-temperature peak becomes larger because there is almost no lower-temperature peak to activate the consumption of bulk lattice oxygen at lower temperature, the latter being similar to the case that shared oxygen species can be reduced at lower temperature [17]. Nevertheless, the total concentration of bulk lattice oxygen is high enough and thus the hydrogen consumption rates during the isothermal period for first and second TPR runs are about the same.

Figure 4 shows that, with a multi-stepped operation, the TPR profile shows a continuously decreasing trend during the three isothermal periods. That is, after a TPR peak was formed with programmed temperature increase, the hydrogen consumption rate during the following isothermal period shows a continuation from the previous isothermal period. This indicates that both the mobility and the concentration of bulk lattice oxygen affect the hydrogen consumption rate. Notably, additional TPR peak is formed due to increased oxygen mobility at higher temperature. The

**Fig. 4** Multi-stepped H<sub>2</sub>-temperature-programmed reduction profile of GDC

behavior of the slowly decreasing hydrogen consumption rate during the isothermal period is the same as the above-described slowly decreasing CO formation rate, which has been attributed to the effect of the concentration of bulk lattice oxygen.

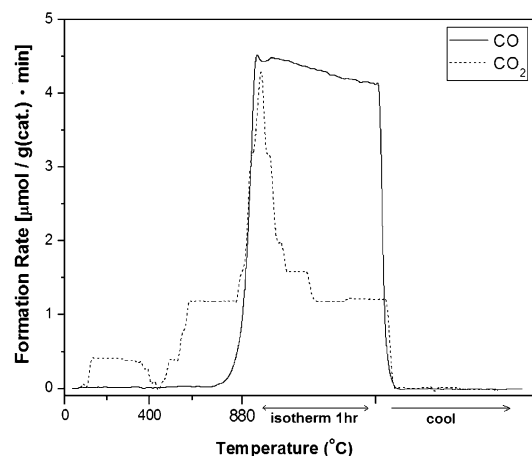
Although the lower-temperature peak during the second TPR run is almost negligible, there is still some H<sub>2</sub> consumption at the lower temperature range, indicating the existence of some surface lattice oxygen species. This is due to the movement of bulk lattice oxygen to the surface and near the surface during the isothermal period of the first TPR run. This is in agreement with the result of temperature-programmed reaction of methane over GDC pre-reduced at 700 °C for 12 h, as shown in Fig. 5 and will be discussed in the following.

### 3.3 Variation of Concentration of Bulk Lattice Oxygen

The concentration of bulk lattice oxygen is varied by varying the temperature and the duration of the pre-reduction treatment. Notably, the supply rate of oxygen species from the bulk onto the surface depends on the mobility and the concentration of bulk lattice oxygen; this oxygen supply rate affects the rate of methane oxidation and thus the rates of CO<sub>2</sub> and CO formations.

#### 3.3.1 CO<sub>2</sub> Formation

Figure 2 shows that, over GDC pre-reduced at 700 °C for 1 h, CO<sub>2</sub> formation is almost negligible before 800 °C during CH<sub>4</sub>-TPR<sub>x</sub>. However, with the same pre-reduction temperature of 700 °C but with the pre-reduction time increases to 12 h, CO<sub>2</sub> formation starts at very low temperature again, shown in Fig. 5. This is attributed to that, although 700 °C pre-reduction consumes some lattice

**Fig. 5** Temperature-programmed reaction of methane over GDC pre-reduced at 700 °C for 12 h

oxygen species, the long stay at 700 °C leads to intensive movement of the bulk lattice oxygen towards the surface. Consequently, enough oxygen species can be left at the surface and near the surface at the end of pre-reduction; this means that the active sites of surface lattice oxygen are created again and the surface lattice oxygen of these sites can be replenished quickly; thus, during subsequent CH<sub>4</sub>-TPR<sub>x</sub>, CO<sub>2</sub> formation is activated at a temperature as low as that of unreduced GDC. Notably, 700 °C is lower than the higher-temperature TPR peak temperature of 740 °C for the reduction of bulk lattice oxygen; thus, some surface lattice oxygen can exist.

With the pre-reduction duration kept at 1 h but with the pre-reduction temperature increased to 800 °C, CO<sub>2</sub> formation before 800 °C during CH<sub>4</sub>-TPR<sub>x</sub> occurs very much again, shown in Fig. 6. However, the lowest-temperature CO<sub>2</sub> peak, at below about 400 °C as shown in both Figs. 1 and 5, disappears. Additionally, CO<sub>2</sub> formation starts at a temperature higher than that of the second CO<sub>2</sub> peak for GDC pre-reduced at 700 °C for 12 h. Notably, almost no CO<sub>2</sub> is formed before 750 °C for GDC pre-reduced at 700 °C for 1 h; this is due to a lack of movement of bulk lattice oxygen at 700 °C. This is again the case when the pre-reduction temperature increases further to 900 °C, shown in Fig. 7. These reveals that 800 °C and 900 °C pre-reduction treatments have removed the surface lattice oxygen completely and also consumed the bulk lattice oxygen extensively. Consequently, the concentration of bulk lattice oxygen becomes lower and thus the replenishment of bulk lattice oxygen to the surface becomes slower, shown by the higher temperature for CO<sub>2</sub> formation.

Table 1 indicates that the amount of CO<sub>2</sub> formation increases with increasing the pre-reduction temperature from 700 °C to 800 °C, but decreases with increasing the pre-reduction temperature further to 900 °C. This is similar

to the TPR phenomena shown in Fig. 4 that the TPR peak after temperature programmed to 850 °C becomes bigger and then that to 950 °C becomes smaller.

### 3.3.2 CO Formation

Table 1 reveals also that the amount of CO formation decreases with increasing pre-reduction temperature. This demonstrates that the CO formation rate depends on the concentration of bulk lattice oxygen, which decreases with increasing pre-reduction temperature. It is seen that the amount of CO formation decreases only slightly over GDC pre-reduced at 700 °C in comparison to that unreduced. However, an increase of the pre-reduction temperature to 800 °C greatly decreases the CO formation. This is attributed to the higher-temperature TPR peak being at 740 °C, which corresponds to the reduction of bulk lattice oxygen. In fact, all results of this work indicate that CO formation occurs almost exclusively at temperatures higher than about 750 °C. Thus, it can be proposed that CO formation is associated solely with the oxygen species coming from the bulk lattice during methane reaction.

Figures 6 and 7 show that, during the isothermal period, the CO formation rate can be kept almost constant. This indicates that the CO formation rate is low enough for the concentration of bulk lattice oxygen to be pseudo-constant. Notably, the total amount of CO formation over the 800 °C-reduced GDC is relatively small and that over the 900 °C-reduced GDC is negligibly small in comparison to the total O content in the unreduced GDC. This confirms that CO formation is associated with the bulk lattice oxygen.

Figure 7 shows also that the CO<sub>2</sub> formation rate is always higher than that of CO formation rate, especially during the isothermal period at 880 °C. This is similar to the report of Huang and Huang [10] that, over Ni-GDC

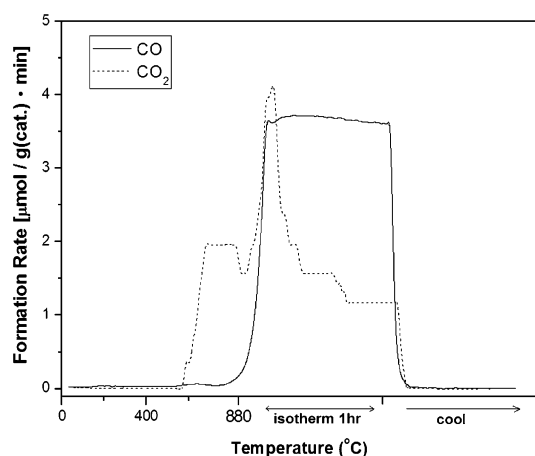


**Fig. 6** Temperature-programmed reaction of methane over GDC pre-reduced at 800 °C for 1 h

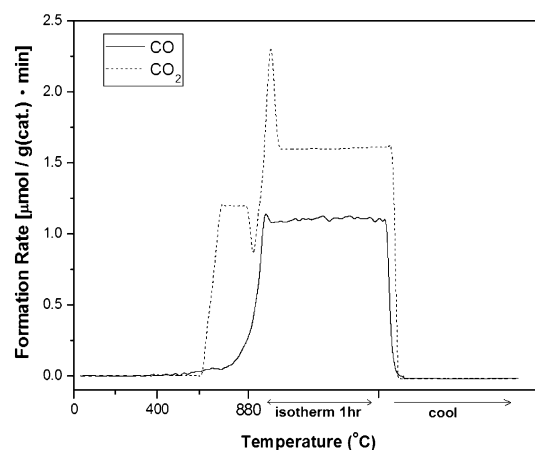


**Fig. 7** Temperature-programmed reaction of methane over GDC pre-reduced at 900 °C for 1 h



anodes in direct-methane solid oxide fuel cells at 800 °C, CO formation rate depends on the oxygen-supply rate to a higher extent than the CO<sub>2</sub> formation rate. Thus, a lowering of the supply rate of bulk lattice oxygen is beneficial to the formation of CO<sub>2</sub> but detrimental to that of CO. Notably, the supply rate of bulk lattice oxygen becomes relatively low due to relatively low concentration of bulk lattice oxygen after 900 °C pre-reduction treatment. This confirms the effect of the concentration of bulk lattice oxygen.

Additionally, Fig. 7 shows also that the CO<sub>2</sub> formation rate is can be kept almost constant. This indicates that the CO formation rate is low enough for the concentration of bulk lattice oxygen to be pseudo-constant.

Therefore, the concentration of bulk lattice oxygen affects the concentration of surface lattice oxygen and consequently influences the reaction pathways of CO and CO<sub>2</sub> formations. Additionally, the nature of oxygen species, i.e., strong or weak bonding to the catalyst surface, may also influence the reaction pathways of CO and CO<sub>2</sub> formations. The mobility of oxygen species may affect their bonding strength to the catalyst surface and thus influences CO and CO<sub>2</sub> formations.

#### 4 Conclusions

- (1) CO<sub>2</sub> formation can occur at very much lower temperature than CO formation.
- (2) The surface lattice oxygen acts as the active site for CH<sub>4</sub> adsorption. This active site has a dynamic characteristic due to that the lattice oxygen is highly mobile at high temperature and able to be supplied from the bulk lattice.
- (3) The rates of CO and CO<sub>2</sub> formations can be controlled by the supply rate of oxygen species from the

bulk lattice; this supply rate depends on both the mobility and the concentration of the bulk lattice oxygen.

- (4) CO<sub>2</sub> formation is associated with the existing surface lattice oxygen.
- (5) CO formation occurs only at temperatures higher than 750 °C and depends completely on the oxygen species coming from the bulk lattice during methane reaction.

#### References

1. Marina OA, Bagger C, Primdahl S, Mogensen M (1999) *Solid State Ionics* 123:199
2. Sauvet al, Fouletier J (2001) *J Power Sources* 101:259
3. Zhu WZ, Deevi SC (2003) *Mater Sci Eng A* 362:228
4. Yaremchenko AA, Valente AA, Kharton VV, Bashmakov IA, Rocha J, Marques FMB (2003) *Catal Commun* 4:477
5. Huang TJ, Wang CH (2006) *J Power Sources* 163:309
6. Lin Y, Zhan Z, Liu J, Barnett SA (2005) *Solid State Ionics* 176:1827
7. Marina OA, Mogensen M (1999) *Appl Catal A: Gen* 189:117
8. Sin A, Kopnin E, Dubitsky Y, Zaopo A, Arico AS, Gullo LR, La Rosa D, Antonucci V (2005) *J Power Sources* 145:68
9. Huang TJ, Wang CH (2007) *Chem Eng J* 132:97
10. Huang TJ, Huang MC (2007) *Chem Eng J* doi:10.1016/j.cej.2007.03.015
11. Murray EP, Tsai T, Barnett SA (1999) *Nature* 400:649
12. Wang JB, Jang JC, Huang TJ (2003) *J Power Sources* 122:122
13. Riess I (2003) *Solid State Ionics* 157:1
14. Marchetti L, Forni L (1998) *Appl Catal B: Environ* 15:179
15. Huang TJ, Yu TC (2005) *Catal Lett* 102:175
16. Huang TJ, Lin HC, Yu TC (2005) *Catal Lett* 105:239
17. Huang TJ, Kung YC (2003) *Catal Lett* 85:49
18. Conesa JC (1995) *Surf Sci* 339:337
19. Xu Y, Lin L (1999) *Appl Catal A: Gen* 188:53
20. Ciuparu D, Pfefferle L (2002) *Catal Today* 77:167
21. Su YS, Ying JY, Green WH Jr (2003) *J Catal* 218:321
22. Laosiripojana N, Assabumrungrat S (2005) *Appl Catal B: Environ* 60:107